Three pulse UV photon echo studies of molecules in solution: Effect of the chirp

A. Ajdarzadeh Oskouei, A. Tortschanoff, O. Bräm, F. van Mourik, A. Cannizzo, and M. Chergui

Citation: The Journal of Chemical Physics **133**, 064506 (2010); doi: 10.1063/1.3463448
View online: http://dx.doi.org/10.1063/1.3463448
View Table of Contents: http://scitation.aip.org/content/aip/journal/jcp/133/6?ver=pdfcov
Published by the AIP Publishing

Three pulse UV photon echo studies of molecules in solution: Effect of the chirp

A. Ajdarzadeh Oskouei, A. Tortschanoff,[a] O. Bräm, F. van Mourik, A. Cannizzo, and M. Chergui[b]

Laboratoire de Spectroscopie Ultrarapide, ISIC, FSB, Ecole Polytechnique Fédérale de Lausanne (EPFL), Station 6, CH-1015 Lausanne, Switzerland

(Received 22 February 2010; accepted 22 June 2010; published online 11 August 2010)

We report on the electronic dephasing times of the nonpolar chromophore diphenylacetylene (DPA) in ethanol and in cyclohexane (polar and nonpolar solvents respectively) by photon echo measurements in the ultraviolet. Contrary to previous reports, we observed sub-100-fs electronic dephasing times for DPA in both solvents. We identify fast dynamics of $\tau = 40 \pm 10$ fs on the photon echo peak shift (PEPS) traces of DPA in ethanol. In addition, we observed a dependence of the PEPS asymptotic value on the temporal chirp of the pulses. We propose a model to describe it in terms of phase-matching condition and beam geometry. © *2010 American Institute of Physics*. [doi:10.1063/1.3463448]

I. INTRODUCTION

The photon echo peak shift (PEPS) technique is a powerful method to investigate intramolecular dephasing processes such as internal vibrational redistribution (IVR) as well as solvation dynamics by tracking the transition frequency correlation function of the chromophore probe.[1–4] It has successfully been employed in the visible and infrared ranges to study solvation and protein dynamics.[5–10] There are interests to extend it to the ultraviolet (UV) range, as aromatic amino-acid residues (tryptophan, phenylalanine, and tyrosine) which are naturally present in most of the proteins, absorb in the UV below 300 nm.[11] The extension of the PEPS technique to this spectral range would allow us to investigate local dynamics in biological systems.[12–15] This is also useful for solvation dynamics studies and, in particular, the study of polar versus nonpolar solvation dynamics as it would allow using UV dyes which are typically smaller and simpler molecules.[16–18] However, there are several aspects that make the PEPS experiment in the UV a difficult task: (1) Nonresonant third-order signals from the solvent become more and more important as we approach the absorption threshold of the solvents.[19] (2) The phase-matching condition is stricter; therefore, sensitivity to the beam geometry is higher. (3) Scattered light is stronger. (4) Third and higher order group velocity dispersions are more pronounced.

These difficulties have prevented photon echo (PE) experiments from being implemented in the UV range, and only the work of Fayer and co-workers[19] existed prior to our studies.[20,21] They investigated the dephasing time of the diphenylacetylene (DPA) in cyclohexane with a two-pulse photon echo technique, and estimated it to be 500 fs using a pulse length dependent theoretical method. Despite a good temporal resolution [full width at half maximum (FWHM) ≈ 80 fs], they could not measure the dephasing time directly because of the presence of the nonresonant signal from the solvent. Their experiment was, indeed, limited to the two-pulse PE scheme with only one degree of freedom for the time ordering of the pulses. In a three-pulse PE setup, two degrees of freedom are available for the time ordering of the pulses. One could place the third pulse out of the overlap region of the first and second pulses (see Fig. 1) in order to eliminate the nonresonant signal from the solvent. In addition, our setup achieves better temporal resolution (FWHM ≈ 50 fs). This allowed us to measure sub-100-fs dephasing times for solutions of p-terphenyl (pTP), 2.5-diphenyloxazole, and tryptophan in polar and nonpolar solvents.[20,21] In the present contribution, we report on results of PE experiments on DPA in ethanol and in cyclohexane (polar and nonpolar solvents, respectively), which differ from those of Fayer and co-workers.[19]

Several articles have reported a depletion or recurrence of the PEPS traces in the visible at short population times ($T_{23} < 100$ fs).[22–26] In addition, a variable nonzero asymptotic value (offset) for the PEPS traces was observed.[26,27] Various explanations have been proposed for these effects, mainly relating them to the specific physical system under study or to interference between the signals from the solute and the solvent. We reported similar effects in our preliminary UV PE studies.[20,21] Since they are observed in various molecular solutions and even in pure solvent (see Sec. III), doubts arise as to a solute-related origin. In addition, they were found to depend on the experimental conditions and, in particular, on the chirp of the pulses.[21] Here, we demonstrate that the origin of these effects is due to the chirp of the pulses. This lifts a long standing ambiguity and provides a basis for future work.

In the first part of this article we present the results of our PE experiments on DPA in solution. In the second part of the article, we discuss the dependence of PEPS traces on the

[a]Present address: CTR Carinthian Tech Research AG, Europastrasse, 4/1, 9524 Villach/St. Magdalen, Austria.
[b]Electronic mail: majed.chergui@epfl.ch.

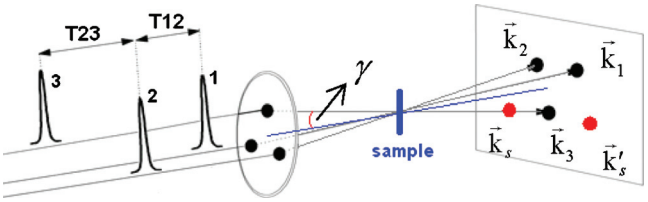

FIG. 1. Triangular geometry of the input beams in the PE setup. The PE signals are detected in two phase-matched directions, $\vec{k}_s=-\vec{k}_1+\vec{k}_2+\vec{k}_3$ and $\vec{k}'_s=-\vec{k}_2+\vec{k}_1+\vec{k}_3$.

chirp of the pulses. Finally we present a model to explain this dependence relating it to the phase mismatch that is present in triangular geometry.

II. UV PE EXPERIMENTS ON DPA

The experimental PE setup was described in detail in Ref. 21. The main difference here is that we use a prism pair compression stage to obtain UV pulses with FWHM of 50–60 fs on the sample at 287 nm, and a spectral width of 3–4 nm. This allows a fine optimization of the chirp of the UV pulses. In addition, we work at a pulse repletion rate of 30 kHz and we use a sample jet with a 100 μm thickness which delivers a stable flow with a speed of about 2 m/s. This allows us (given the beam diameter of about 50 μm on the sample) to refresh the sample after each laser pulse in order to rule out any thermally cumulative or reabsorption effects.

The PEPS value for a given T_{23} is, by definition, the value of T_{12} where the maximum of the PE signal appears. In the standard approach that is based on the triangular geometry of the beams (Fig. 1), the PE signal is detected in two symmetric phase-matched directions of $-\vec{k}_1+\vec{k}_2+\vec{k}_3$ and $-\vec{k}_2+\vec{k}_1+\vec{k}_3$, while scanning pulses 1 and 2 with respect to each other for a fixed T_{23}. The PEPS value is calculated as half the time difference between the signal peaks in these two directions.[2,22] As an example, Fig. 2 shows the PE signals detected in two phase-matching directions at $T_{23}=1$ ps, showing a measured PEPS equal to 18 fs. Performing the same scans for different values of T_{23}, one gets the PEPS trace for the given sample.

The great advantage of the triangular beam geometry is the symmetric distribution of signals. This delivers subfemtosecond resolution for the PEPS measurements at the cost of a less efficient PE signal generation due to a nonperfect phase-matching.[2,22] However, the main drawback of this geometry is, as shown later, that it causes a dependence of the PEPS trace on the chirp of the pulses.

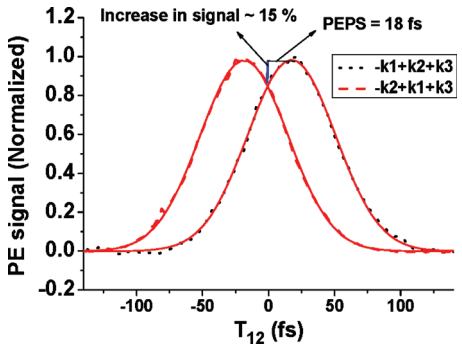

FIG. 2. An example of the PE signals detected in two phase-matched directions at $T_{23}=1$ ps. The PEPS value is measured to be 18 fs. The maximum of signal is about 15% higher than the signal value at $T_{12}=0$.

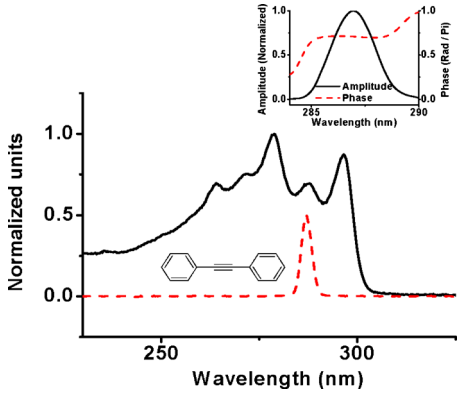

FIG. 3. Absorption spectrum of DPA (see scheme of the molecular structure) in ethanol (solid black line) and the excitation pulse spectrum (dashed red line). Inset: spectral amplitude and phase of the UV pulses at the sample position.

The absorption spectrum and the molecular structure of DPA are shown in Fig. 3, along with a typical excitation pulse spectrum. We show in the inset the spectral amplitude and phase of the UV pulses retrieved by the frequency resolved optical gating (FROG) technique.[28–30] Indeed, the constant phase of the electric field at the sample position points out to an excellent level of chirp compensation we achieved with the UV prism-based compression stage. We performed PE experiments on DPA in ethanol and cyclohexane and compared them with the PE signal of pTP in ethanol and that of pure ethanol, where only sub-100-fs dephasing time and pure nonresonant signals are respectively present.[20,21,31,32] Figure 4 shows the PE signals from DPA in ethanol and cyclohexane, pTP in ethanol, and the pure solvent, detected in the phase-matching direction $-\vec{k}_1+\vec{k}_2+\vec{k}_3$, by scanning T_{12} at $T_{23}=0$ and $T_{23}=100$ fs. One should note that in the case of Fig. 4(b) ($T_{23}=100$ fs), there is no considerable overlap of the third pulse with the others. Therefore the nonresonant signal from the solvent is negligible, and the detected signal entirely comes from the solute. In this case, we can measure the dephasing times of the solute molecule without artifacts from the solvent.[19] Any detectable dephasing time would lead to an asymmetry in the signals. However, all the signals in Fig. 4 are symmetric and almost identical. As a result, within our time resolution, DPA in ethanol and in cyclohexane do not show any detectable dephasing time and we conclude that the electronic dephasing time of nonpolar chromophore DPA in both polar and nonpolar solvents is sub-100-fs. We note in Fig. 4(a) a tiny difference in the wings between the signal of the pure solvent and that of DPA and pTP solutions. The signals from DPA and pTP are longer and we explain this as an effect of the additional group velocity dispersion induced by the absorbing solute molecule. It should be noted that in Fig. 4, T_{12}' is not identical to T_{12}; indeed, the signals are shifted to have the maxima at $T_{12}'=0$. The position of T_{12} at which the maxi-

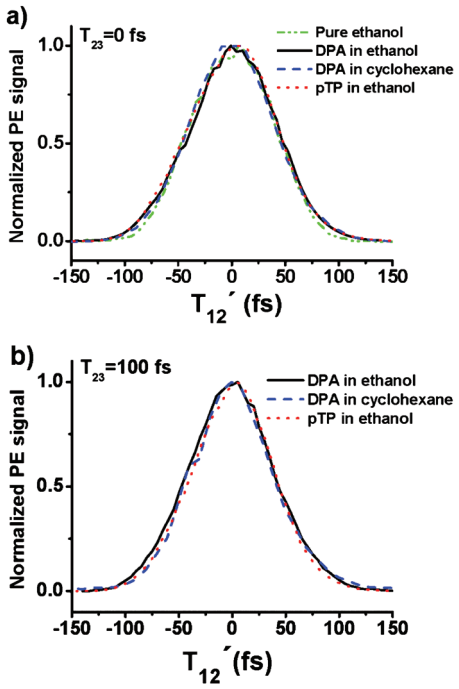

FIG. 4. PE signals for DPA in ethanol (solid black line), DPA in cyclohexane (dashed blue line), pTP in ethanol (dotted red line) and pure ethanol (dashed-dotted green line), detected in the phase-matching direction $-\vec{k}_1+\vec{k}_2+\vec{k}_3$ at (a) $T_{23}=0$ and (b) $T_{23}=100$ fs. Signals are shifted to overlap their maxima at $T_{12}'=0$.

mum of the signal occurs, is equal to the PEPS value and as will be discussed in the next section, its absolute value in UV experiments depends on experimental conditions.

The present results are different from those of Fayer and co-workers.[19] As already mentioned, their setup was based on the two-pulse PE scheme. In this scheme, one does not separate temporally the third pulse from the others, in other words, $T_{23}=0$ always. In this case, the nonresonant signal from the solvent is always present and introduces artifacts in the measurement of the dephasing time. As a result, they were not able to measure directly the dephasing time and they estimated it using a pulse length dependent theoretical method. In addition, in a theoretical work on the dephasing times of nonpolar solutes in nonpolar solvents, which was investigated by simulation of the photon echo signal,[33] the electronic dephasing was found to originate primarily from the slight rearrangement of the first solvation shell around the chromophore. The decay of the photon echo signal and consequently the dephasing time calculated using this model is in agreement with the results obtained by Fayer and coworkers. However, our experiment revealed that electronic dephasing occurs on much shorter time scales, excluding that the dephasing is caused by the first solvent shell rearrangement. Instead, this speaks for a much faster, probably intramolecular, dephasing mechanism. In this respect, we recently reported sub-50-fs intramolecular dynamics due to internal conversion (IC) and IVR, in a large variety of systems.[20,34–39] Therefore, we tentatively propose that the primary mechanisms for electronic dephasing here are IC and IVR.

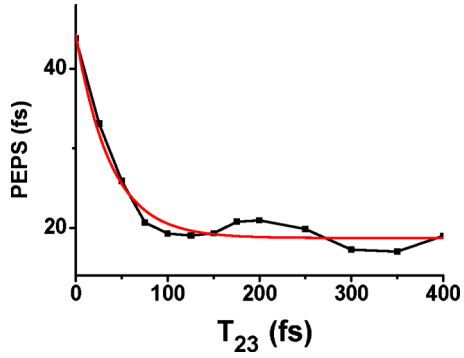

FIG. 5. PEPS trace of DPA in ethanol, fitted by a monoexponential decay plus an offset.

Indeed, the width of vibronic bands in Fig. 3 corresponds to the total dephasing rate (homogeneous dephasing plus inhomogeneous dephasing) of the system. By fitting the first band at 296.5 nm with a Gaussian lineshape, we find a FWHM of about 800 cm^{-1}, which corresponds to a dephasing time of about 6–10 fs. Important to note is that any attempt to use a Lorentzian profile to fit the band was unsuccessful. We can therefore estimate that the inhomogeneous (Gaussian) broadening is at least three to four times larger than the homogeneous (Lorentzian) one, and we deduce that the homogeneous dephasing time should not be lower than about 20 fs. We can thus set lower and upper limits of 20 and 100 fs, respectively, for the homogeneous dephasing time of DPA in solution.

A measured PEPS trace of DPA in ethanol fitted with a monoexponential decay plus an offset is shown in Fig. 5. We obtain a decay time of $\tau=40\pm10$ fs for the PEPS trace. Rather similar decay times were reported previously in the PEPS and the time-resolved fluorescence experiments on various dyes in ethanol in the visible range.[40,41] Ultrafast dynamics in this range are originated either by intramolecular dephasing processes or by spectral diffusion as a result of the solvent reaction (as ethanol is a polar solvent). The offset value depends on experimental conditions and, as discussed in the next section, is not related to solute or solvent properties.

III. DEPENDENCE OF THE PEPS TRACES ON THE CHIRP

Figure 6 shows an example of the dependence of the offset value of the PEPS on the temporal chirp for DPA in ethanol. In general, we find that the variation range of the PEPS offset caused by the chirp is in the order of ±20 fs. The expected dynamics on PEPS traces is also normally in the range of few tens of femtoseconds (e.g., as seen in Fig. 5).

A similar behavior is also observed in pure solvents. Figure 7 shows the signals from pure ethanol in two phase-matched directions where we set $T_{23}=0$ and we scan T_{12} (see Fig. 1). The origin of this nonresonant signal is the instantaneous response of the electronic polarizability of the solvent. Accordingly, its intensity should be proportional to the overlap of the three pulses. In particular, the signal intensity should be maximal at $T_{12}=0$ while having $T_{23}=0$. On the

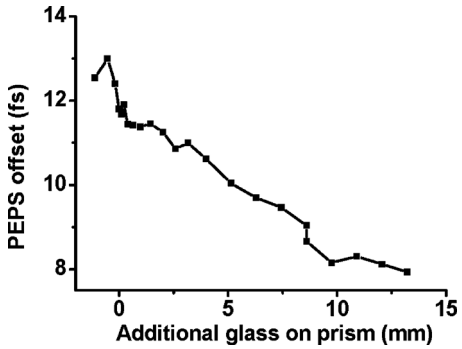

FIG. 6. An example of dependence of the PEPS offset on the chirp, obtained by increasing the length of glass in the compression stage prism through which the beam passes. The measurements were done on DPA in ethanol. (T_{23}=1 ps).

contrary, the maximum of experimental signals in the two phase-matching directions ($-\vec{k}_1+\vec{k}_2+\vec{k}_3$ and $-\vec{k}_2+\vec{k}_1+\vec{k}_3$) do not occur at T_{12}=0 and they are shifted in opposite T_{12} directions. This would correspond to a nonzero PEPS. Indeed the latter is defined for the resonant PE signals. In the case of pure solvent, there is no coherence and population times and the PEPS is not defined. Here we mean that the shift of the nonresonant signal is equivalent to the nonzero PEPS value. We also observed that the magnitude of this shift depends on the pulse chirp. This result in the pure solvent rules out any solute-related mechanism. One should note that this shift is not an effect of the uncertainty on the determination of time zero; otherwise, both phase-matched signals would have been shifted in the same T_{12} direction.

IV. DISCUSSION

The dependence of the PEPS on the temporal chirp speaks for a mechanism that concerns the relative time ordering of the different spectral components of the pulse. Figure 8 shows the pictorial representation of the situation where we have chirped pulses that interact with each other at a nonzero T_{12}. It is clear that different spectral components from the first and second pulses overlap with each other. In order to verify if this would be the origin of the PEPS dependence, we reviewed the role of nonperfect phase-matching in the here adopted triangular geometry (Fig. 1) on the PE signal.

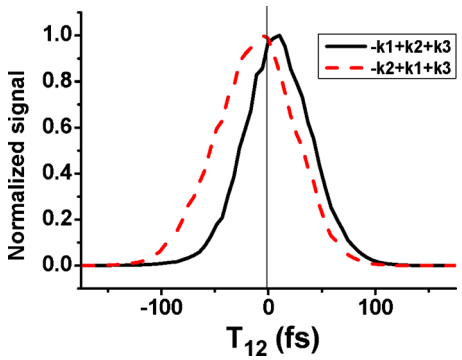

FIG. 7. Nonresonant signal from pure ethanol in two phase-matched directions (T_{23}=0).

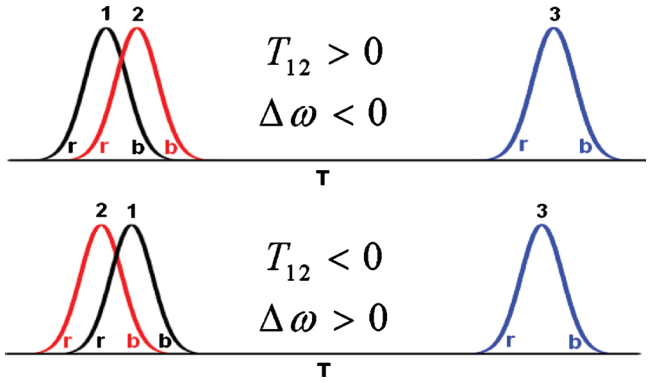

FIG. 8. Interaction of chirped pulses in the PE setup. In this scheme, pulses are positively chirped. "r" refers red chirp and "b" refers to blue chirp of the pulses. $\Delta\omega$ is the average detuning of the interacting components of the first and second pulses from ω_0 defined by Eq. (2).

One can calculate the amount of phase mismatch that is present in a given geometry of the beams by considering the two conditions of "wave vector" and "frequency" matching,

$$\vec{k}_s = -\vec{k}_1 + \vec{k}_2 + \vec{k}_3,$$
$$\omega_s = -\omega_1 + \omega_2 + \omega_3, \tag{1}$$

where $\omega_1, \omega_2, \omega_3$ and $\vec{k}_1, \vec{k}_2, \vec{k}_3$ are the interacting frequencies and wave vectors of the first, second, and third pulses, respectively. Here we consider the simpler case where the three pulses are identical and symmetrical, with the same time ordering of the frequency components at the sample position. In this case, we can rewrite the interacting frequencies of the first and second pulses, which are temporally overlapped as follows:

$$\omega_1 = \omega_0 - \Delta\omega, \quad \omega_2 = \omega_0 + \Delta\omega, \tag{2}$$

where ω_0 is the central frequency of the pulses and $\Delta\omega$ is the average detuning of the interacting components of the first and second pulses from ω_0. $\Delta\omega$ depends on T_{12} and becomes zero at T_{12}=0. In addition, we have $\omega_3=\omega_0$ because the system interacts with the entire frequency components of the third pulse. The phase mismatch is defined as[42]

$$\Delta k = |\vec{k}_s| - \frac{\omega_s}{c}. \tag{3}$$

In triangular geometry, it can be calculated to be

$$\Delta k = \frac{1}{c}\{[\omega_0^2 + \cos^2\gamma\,(4\Delta\omega^2 + 4\omega_0\Delta\omega) + \sin^2\gamma\,(3\omega_0^2 + \Delta\omega^2 - 2\omega_0\Delta\omega)]^{1/2} - \omega_0 - 2\Delta\omega\,.\} \tag{4}$$

Here γ is the angle between the input beams and the horizontal axis (see Fig. 1). In the noncollinear geometry γ is nonzero; therefore, Δk is always nonzero. The nonzero mismatch causes a decrease of nonlinear signal intensity as will be discussed later [Eq. (5)]. In Fig. 9, we plot the phase mismatch as a function of $\Delta\omega$ using Eq. (4). Here, we used experimental parameters (beam angle γ=3.1° and λ =287 nm). One may note that for a typical bandwidth of the

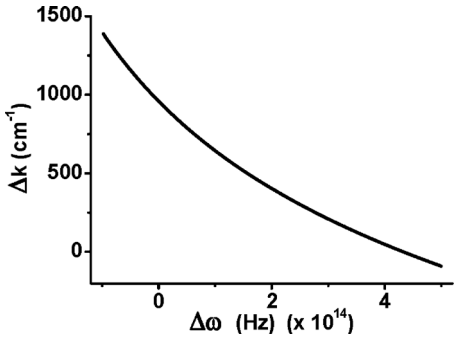

FIG. 9. The phase mismatch (Δk) as a function of $\Delta\omega$ in the triangular geometry (γ=3.1° and λ=287 nm).

input pulses ($\Delta\lambda \cong 4$ nm in our experiment), one can only have $\Delta\omega$ in the order of $10^{12}-10^{13}$ Hz that delivers a small change in the total amount of Δk (variations less than 3%). However, we show in the following that this is sufficient to cause the observed variations in the PEPS offset.

The third order nonlinear signal intensity in the approximation of nondepleted pump is given by[42]

$$I_s \propto \mathrm{L}^2\left[\mathrm{sinc}\left(\frac{\Delta \mathrm{kL}}{2}\right)\right]^2. \tag{5}$$

Here L is the sample thickness. We show in the Appendix that there is no significant difference between the nondepleted pump approximation (no absorption of the input pulses) and our experimental case where samples with optical density (OD) of about 0.3 OD were used.

Figure 10 shows the normalized profiles of I_s given by Eq. (5). Considering our experimental conditions (λ=287 nm, beam angle of γ=3.1°, and the sample thickness of L=100 μm), experimental range of $\Delta k \times L$ is in the region marked in the inset of Fig. 10. As can be seen, in this case the intensity of the generated nonlinear signal is about 5% of the signal intensity for the case of perfect phase-matching. It is evident that for the nonchirped condition, we always have $\Delta\omega$=0. In this case, the nonzero mismatch just results in a reduction of the output signal. However, for the case of chirped pulses, as shown in Fig. 8, $\Delta\omega$ and therefore the amount of phase mismatch (Δk) changes by varying T_{12}. This implies, considering Figs. 9 and 10, that we will have better phase-matching conditions and therefore, stronger signals at some nonzero values of T_{12} (positive or negative

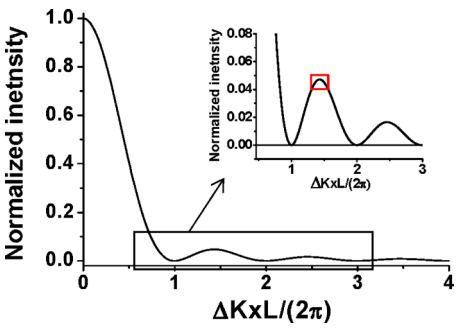

FIG. 10. Normalized intensity of nonlinear signal as a function $\Delta kL/2\pi$ given by Eq. (5). Inset: the range of possible values of $\Delta k \times L$ given by our experimental conditions is marked by a small red square.

value). This increase of the signal will compete with a decrease of signal due to a smaller pulse overlap. Consequently, there is a particular nonzero value of T_{12} where the maximum of the PE signal is generated and this appears as a nonzero PEPS offset. Remarkably, this nonzero PEPS is due to the pulse chirp and not to the dynamics of the system under study. Considering Eq. (2) and Figs. 8 and 9, and assuming a positive temporal chirp for the light pulses, when the slope of the I_s is negative in Fig. 10 at a given experimental value of $\Delta k \times L$, better phase-matching and stronger signals occur in $T_{12}<0$ and we obtain a negative PEPS offset. However, when its slope is positive, better phase-matching and stronger signals occur for $T_{12}>0$ and we get a positive PEPS offset.

For the experimental range of $\Delta k \times L$ given in the inset of Fig. 10, according to Eq. (5), small changes in Δk as given by the pulse bandwidth $\Delta\lambda \cong 4$ nm and Eq. (4), can cause an increase of about 5%–20% in the signal, which is sufficient to have a variation of the PEPS offset of the order of $\pm$20 fs. For example, in our experimental data of the PE signal in Fig. 2, the measured PEPS is equal to 18 fs and at T_{12} =18 fs, the signal increases by about 15% compared to the signal at T_{12}=0. This increase can certainly be generated by variation of Δk caused by the chirp. For the same reason, the pure solvent signals are shifted out of the exact zero time in Fig. 7.

We should note that at the higher frequencies, we have a greater phase mismatch according to Eq. (4). Therefore the PEPS dependence on the chirp is more pronounced than in the case of UV pulses than for IR or visible pulses.

The above discussion also explains the observation of depleted PEPS traces in the overlap region for the case of chirped pulses.[21] Indeed in the overlap region, three pulses overlap with each other and a strong nonresonant signal is generated in addition to the PE signal. The intensity of the nonresonant signal also depends on the phase-matching; therefore in the overlap region, PEPS is more sensitive to the chirp.

We found out that the PEPS offset also depends on the alignment of the beams on the sample. Indeed, by altering the alignment, we change γ and therefore, the mismatch (Δk) changes according to Eq. (4). Therefore, the experimental value of $\Delta k \times L$ in Fig. 10 changes and as a result, the chirp-dependent PEPS offset also changes. We calculated, based on Eqs. (4) and (5), that a change of 0.1° in the beam angle (γ) can cause a change of the PEPS value in the order of $\pm$20 fs. In addition, in the case of spatial chirp of the beams that can be caused by nonperfectly aligned Optical Parametric Amplifiers (OPA) or Non-collinear Optical Parametric Amplifiers (NOPA), by altering the alignment of the beams, we also modify the interacting frequency components and subsequently the Δk; therefore, the PEPS offset changes. Similar discussions can explain the dependence of the PEPS offset on the sample thickness, as already observed.[21,26] Here as L changes, the experimental value of $\Delta k \times L$ changes, which delivers a different chirp induced PEPS offset value.

Considering such effects of the experimental conditions, in particular, the chirp of the pulses, the question arises whether the PEPS measurements in the UV are reliable. We

note that the dependence of the offset value of the PEPS on the experimental conditions does not mean that the dynamics observed on the PEPS trace is meaningless. Indeed when we keep the experimental parameters constant and, in particular, when we minimize and fix the chirp of the pulses during the measurement, we always obtain the same dynamics on the PEPS traces. Therefore, the dynamics therein reported are reliable, but not their offset values.

As far as the effect of the group velocity dispersion through the sample is considered, we used a sample thickness of 100 μm to minimize it. In addition, we checked with different sample thicknesses (100, 200, and 500 μm) and we observed that the sample thickness has no effect on the time resolution of the experiment, considering that we minimize the chirp of the UV pulses at the sample position by prism pair compression stage.

We should note that in real conditions, the temporal and spatial chirps can hardly be eliminated. However, in our setup, which employs a prism-based compression stage and rather narrow bandwidths; we achieved a satisfactory minimization of the chirp as proven by the phase of electric field shown in Fig. 3 and confirmed by the lack of time-zero PEPS depletion. More sophisticated methods such as pulse shaping or use of deformable mirrors would be likely necessary for broader pulses. We characterized the time structure of the pulses not only with pulse autocorrelation but also with the FROG technique,[28–30] which retrieves the amplitude and phase of electric field as nicely shown in Fig. 3. The possibility to monitor the phase, which has a high sensitivity to the pulse chirp, allows us to make a better optimization of the chirp than adopting autocorrelation-based technique. As a general comment, the control of the pulse chirp, alignment, and other experimental parameters is critical during the PEPS experiments in the UV to avoid artifacts which may be confused with real dynamics.

V. CONCLUSIONS

In this paper we presented the results of PE experiments on DPA in ethanol and in cyclohexane (polar and nonpolar solvents, respectively). Sub-100-fs electronic dephasing times were observed in both solvents. This result contradicts models proposing that only the solute-solvent interactions play a major role in electronic dephasing[33] and as a result, the dephasing times in the case of nonpolar solvation are longer. This suggests that for a nonpolar solute in a nonpolar solvent, the electronic dephasing originates primarily from intramolecular dynamics and, in particular, IC and IVR. We identified a fast dynamics of $\tau=40\pm10$ fs on the PEPS trace of DPA in ethanol which is close to the decay times observed in the previous works on various dyes in ethanol. It can be originated either by intramolecular dephasing processes or by solvent caused by spectral diffusion, as ethanol is a polar solvent.

We discussed the dependence of PEPS traces on the chirp of the pulses in the case of nonperfect phase-matching, in particular, the case of triangular geometry. We described how the chirp can change the offset value of the PEPS and how it can introduce depletion on the PEPS trace. We explained why these effects are more pronounced in the UV range, compared to the visible or IR ranges. We concluded that in order to obtain reliable PEPS dynamics in the UV range, one should have a high control on the experimental parameters, in particular the chirp of the pulses.

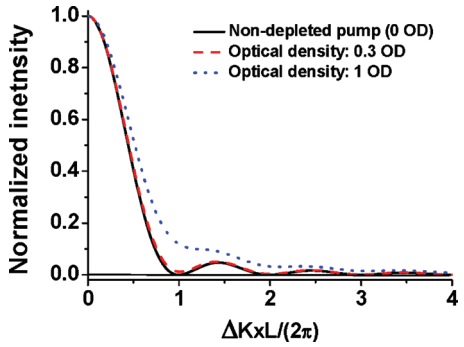

FIG. 11. Normalized intensity of nonlinear signal as a function $\Delta kL/2\pi$ for the case of 0.3 OD (real condition, dashed red line), 0 OD (nondepleted pump, solid black line), and 1 OD (dotted blue line).

ACKNOWLEDGMENTS

This work was supported by the Swiss National Science Foundations (FNS) via contract No. 200020_121839.

APPENDIX: EFFECT OF OPTICALLY DENSE SAMPLE

In our discussion in Sec. IV, we used the nondepleted pump approximation [Eq. (5)] where we assume that the intensity of input pulses is constant through the sample. However, we normally use concentrated samples with an optical density of about 0.3 OD; therefore, the pulses are absorbed and their intensities are not constant through the sample. In order to have exact results, one should extend Eq. (5) to the case of depleted pump pulses by including the effect of absorption of the input pulses as well as the absorption of the generated PE signal within the sample. We begin with the differential equation of the signal field taking into account the absorption,[42,43]

$$\frac{\partial E_s(z)}{\partial z} = ik_s(E_{\text{in}}e^{-\alpha z})^3\exp(i\Delta kz) - \alpha E_s(z). \tag{A1}$$

Here, E_s is the electric field magnitude of the PE signal and E_{in} is the electric field magnitude of the input beam. α is the attenuation factor of the sample. For a sample concentration of 0.3 OD with the thickness of $L=100$ μm, we have $\alpha=3465$. By solving Eq. (A1), we get an expression for the intensity of the nonlinear signal for the case of depleted pump,

$$I_s = \frac{nck_s{}^2E_{\text{in}}{}^6e^{-2\alpha L}}{2\pi(4\alpha^2+\Delta k^2)}\left(1+e^{-4\alpha L}-2e^{-2\alpha L}\cos(\Delta kL)\right). \tag{A2}$$

One may compare the difference between I_s as a function of Δk for the nondepleted and the depleted pump conditions, respectively, given by Eqs. (5) and (A2). Figure 11 shows the normalized profiles of I_s for the case of 0.3 OD (realistic condition), and for two extreme cases of the nondepleted pump (0 OD), and 1 OD. It is evident that there is no sig-

nificant change between 0.3 OD case and the nondepleted case; therefore, one may use Eq. (5) with a good accuracy for the realistic case of 0.3 OD. As the result, our discussion above about the effects of the chirp is valid.

However, as a remark, the I_s profile for the extremely depleted case of 1 OD is significantly different from the other two profiles and tends to be monotonic. It may be the reason why in Ref. 26, a depletion (recurrence) was observed in the lower ODs which disappeared in the higher ODs. In the case of higher ODs, the slope of I_s versus $\Delta k \times L$ becomes smaller; therefore, according to the discussion above, the sensitivity of the PEPS to the chirp gets weaker and weaker; consequently, the depletion, which is originated by the chirp, disappears.

[1] T. H. Joo, Y. W. Jia, J. Y. Yu, M. J. Lang, and G. R. Fleming, J. Chem. Phys. **104**, 6089 (1996).
[2] W. P. de Boeij, M. S. Pshenichnikov, and D. A. Wiersma, J. Phys. Chem. **100**, 11806 (1996).
[3] M. H. Cho, J. Y. Yu, T. H. Joo, Y. Nagasawa, S. A. Passino, and G. R. Fleming, J. Phys. Chem. **100**, 11944 (1996).
[4] W. P. de Boeij, M. S. Pshenichnikov, and D. A. Wiersma, Chem. Phys. Lett. **253**, 53 (1996).
[5] W. P. de Boeij, M. S. Pshenichnikov, and D. A. Wiersma, Annu. Rev. Phys. Chem. **49**, 99 (1998).
[6] S. A. Passino, Y. Nagasawa, T. Joo, and G. R. Fleming, J. Phys. Chem. A **101**, 725 (1997).
[7] R. Agarwal, B. S. Prall, A. H. Rizvi, M. Yang, and G. R. Fleming, J. Chem. Phys. **116**, 6243 (2002).
[8] P. Hamm, M. Lim, W. F. DeGrado, and R. M. Hochstrasser, J. Phys. Chem. A **103**, 10049 (1999).
[9] K. Ohta and K. Tominaga, Bull. Chem. Soc. Jpn. **78**, 1581 (2005).
[10] B. M. Cho, C. F. Carlsson, and R. Jimenez, J. Chem. Phys. **124**, 144905 (2006).
[11] J. R. Lakowicz, *Principles of Fluorescence Spectroscopy*, 3rd ed. (Springer, New York, 2006).
[12] S. Schenkl, F. van Mourik, G. van der Zwan, S. Haacke, and M. Chergui, Science **309**, 917 (2005).
[13] L. Y. Zhang, Y. T. Kao, W. H. Qiu, L. J. Wang, and D. P. Zhong, J. Phys. Chem. B **110**, 18097 (2006).
[14] J. H. Xu, D. Toptygin, K. J. Graver, R. A. Albertini, R. S. Savtchenko, N. D. Meadow, S. Roseman, P. R. Callis, L. Brand, and J. R. Knutson, J. Am. Chem. Soc. **128**, 1214 (2006).
[15] J. Leonard, E. Portuondo-Campa, A. Cannizzo, F. van Mourik, G. van der Zwan, J. Tittor, S. Haacke, and M. Chergui, Proc. Natl. Acad. Sci. U.S.A. **106**, 7718 (2009).
[16] B. M. Ladanyi and R. M. Stratt, J. Phys. Chem. **100**, 1266 (1996).
[17] A. C. Yu, C. A. Tolbert, D. A. Farrow, and D. M. Jonas, J. Phys. Chem. A **106**, 9407 (2002).
[18] D. S. Larsen, K. Ohta, and G. R. Fleming, J. Chem. Phys. **111**, 8970 (1999).
[19] D. Zimdars, R. S. Francis, C. Ferrante, and M. D. Fayer, J. Chem. Phys. **106**, 7498 (1997).
[20] A. Ajdarzadeh Oskouei, O. Bräm, A. Cannizzo, F. van Mourik, A. Tortschanoff, and M. Chergui, Chem. Phys. **350**, 104 (2008).
[21] A. Ajdarzadeh Oskouei, O. Bräm, A. Cannizzo, F. van Mourik, A. Tortschanoff, and M. Chergui, J. Mol. Liq. **141**, 118 (2008).
[22] S. A. Passino, Y. Nagasawa, and G. R. Fleming, J. Chem. Phys. **107**, 6094 (1997).
[23] X. J. Jordanides, M. J. Lang, X. Y. Song, and G. R. Fleming, J. Phys. Chem. B **103**, 7995 (1999).
[24] K. Ohta, D. S. Larsen, M. Yang, and G. R. Fleming, J. Chem. Phys. **114**, 8020 (2001).
[25] R. Jimenez and F. E. Romesberg, J. Phys. Chem. B **106**, 9172 (2002).
[26] N. Christensson, B. Dietzek, T. Pascher, A. Yartsev, and T. Pullerits, Chem. Phys. Lett. **457**, 106 (2008).
[27] T. H. Joo, Y. W. Jia, J. Y. Yu, D. M. Jonas, and G. R. Fleming, J. Phys. Chem. **100**, 2399 (1996).
[28] J. N. Sweetser, D. N. Fittinghoff, and R. Trebino, Opt. Lett. **22**, 519 (1997).
[29] R. Trebino, K. W. DeLong, D. N. Fittinghoff, J. N. Sweetser, M. A. Krumbugel, B. A. Richman, and D. J. Kane, Rev. Sci. Instrum. **68**, 3277 (1997).
[30] D. Lee, S. Akturk, P. Gabolde, and R. Trebino, Opt. Express **15**, 760 (2007).
[31] D. McMorrow and W. T. Lotshaw, J. Phys. Chem. **95**, 10395 (1991).
[32] B. J. Loughnane, A. Scodinu, and J. T. Fourkas, J. Phys. Chem. B **110**, 5708 (2006).
[33] A. M. Walsh and R. F. Loring, Chem. Phys. Lett. **186**, 77 (1991).
[34] A. Cannizzo, O. Bräm, G. Zgrablic, A. Tortschanoff, A. A. Oskouei, F. van Mourik, and M. Cherguil, Opt. Lett. **32**, 3555 (2007).
[35] G. Zgrablic, K. Voitchovsky, M. Kindermann, S. Haacke, and M. Chergui, Biophys. J. **88**, 2779 (2005).
[36] G. Zgrablić, S. Haacke, and M. Chergui, J. Phys. Chem. B **113**, 4384 (2009).
[37] A. Cannizzo, F. van Mourik, W. Gawelda, G. Zgrablic, C. Bressler, and M. Chergui, Angew. Chem., Int. Ed. **45**, 3174 (2006).
[38] W. Gawelda, A. Cannizzo, V. T. Pham, F. van Mourik, C. Bressler, and M. Chergui, J. Am. Chem. Soc. **129**, 8199 (2007).
[39] A. Cannizzo, A. M. Blanco-Rodriguez, A. El Nahhas, J. Sebera, S. Zalis, A. Vlcek, and M. Chergui, J. Am. Chem. Soc. **130**, 8967 (2008).
[40] N. Christensson, B. Dietzek, A. Yartsev, and T. Pullerits, Chem. Phys. **357**, 85 (2009).
[41] M. L. Horng, J. A. Gardecki, A. Papazyan, and M. Maroncelli, J. Phys. Chem. **99**, 17311 (1995).
[42] R. W. Boyd, *Nonlinear Optics*, 2nd ed. (Academic, Amsterdam, 2003).
[43] S. X. Song, C. T. Allen, K. R. Demarest, and R. Q. Hui, J. Lightwave Technol. **17**, 2285 (1999).